3D simulation of macroscopic heat and mass transfer properties from the microstructure of wood fibre networks

Heiko Thoemen, Thomas Walther, Andreas Wiegmann

Accepted Manuscript

3D simulation of macroscopic heat and mass transfer properties from the microstructure of wood fibre networks

Heiko Thoemen, Thomas Walther, Andreas Wiegmann

PII: S0266-3538(07)00409-5
DOI: 10.1016/j.compscitech.2007.10.014
Reference: CSTE 3860

To appear in: *Composites Science and Technology*

Received Date: 25 May 2007
Revised Date: 10 October 2007
Accepted Date: 16 October 2007

Please cite this article as: Thoemen, H., Walther, T., Wiegmann, A., 3D simulation of macroscopic heat and mass transfer properties from the microstructure of wood fibre networks, *Composites Science and Technology* (2007), doi: 10.1016/j.compscitech.2007.10.014

Title:

3D simulation of macroscopic heat and mass transfer properties from the microstructure of wood fibre networks.

Authors:

1. Heiko Thoemen (corresponding author): University of Hamburg, Department of Wood Science, Leuschnerstrasse 91, 21031 Hamburg, Germany, thoemen@holz.uni-hamburg.de, phone +49-40-73962-601, fax +49-40-73962-699
2. Thomas Walther: Voith Paper Technology Center GmbH, Paul-Hartmann-Strasse 4, 89522 Heidenheim, Germany
3. Andreas Wiegmann: Fraunhofer ITWM, Fraunhofer-Platz 1, 67663 Kaiserslautern, Germany

Journal:

Composites Science and Technology

1 Introduction

Heat and mass transfer properties of natural fibre-based materials are needed for a variety of different purposes, including modelling the processing conditions during composites manufacture and characterizing building materials. Typical properties that are required are, among others, permeability and thermal conductivity.

Unlike glass fibres or other synthetic fibre materials, plant fibres in their natural form are of considerable variability. This, together with the diversity of the pulping methods and fibre treatments that may be employed, as well as process fluctuations, add on to the considerable variability of the resulting fibre material.

In order to provide reliable macroscopic heat and mass transfer properties for individual natural fibre-based networks, simple and fast methods are needed to determine these properties. The approach most commonly used is to directly measure them. Methods to characterize building materials are typically described in national or international standards. When using mat property data for process modelling purposes one has to take into account that these data typically depend on the mat density and other internal mat conditions. As these conditions may change over time and space throughout the process, appropriate data are needed that describe the transfer properties as a function of the relevant mat conditions. For example, the thermal conductivity of a wood-furnish material strongly depends not only on its density, but also on its moisture content and temperature. Consequently, for modelling the hot pressing process it is necessary to know the thermal conductivity for the whole density, moisture content and temperature range that locally appears during this process. Fortunately, mat permeability, unlike thermal conductivity, mainly depends on density.

Direct measurements of the permeability as a function of density have been reported, among others, by von Haas *et al.* [1], Garcia and Cloutier [2] and Thoemen

and Klueppel [3], and experimental work to determine the thermal conductivity of wood-furnish mats was done by Shao [4], von Haas [5] and Klueppel [6]. Please note that only those works are listed here where a homogeneous density distribution within the samples were used, which is a requirement to obtain a quantitative relationship between the respective property and density. As panels produced by common methods usually show a pronounced vertical density profile, considerable efforts are facilitated on the manufacture of appropriate testing samples. Given that a homogeneous density profile is used, the experimental approach provides reliable data, but is time consuming, and can, therefore, only be applied to a limited number of different materials.

Another limitation of the experimental approach is that it only provides an empirical link between raw material and processing steps earlier in the process on the one hand, and physical properties on the other hand. However, for a more solid understanding of this relationship it appears to be advantageous to link raw material and process parameters to the structure of the network, and then to relate the structure to the heat and mass transfer properties.

Following this idea some researchers have employed modelling approaches. Such approaches typically combine two independent models, one to link - either directly or indirectly - raw material and earlier processes to mat structure, and one to describe the heat and mass transfer coefficients as a function of mat structure. Such mathematical-physical approach has the advantage of providing fundamental insight into the dependencies between geometrical parameters, for example size and orientation of the individual elements, and the material characteristic of interest.

Dai *et al.* [7] presented a geometrical model for the structure of oriented strand board (OSB) mats, combined with a semi-theoretical model to relate the simplified mat structure to permeability. The latter model is obtained by fitting experimental data to a modified Carman-Kozeny equation that links between-strand porosity and strand

thickness to permeability. Zombori [8] derived the heat transfer properties of OSB mats by first simulating the structure of the mat using a Monte Carlo modelling approach, and then computing its thermal conductivity based on the thermal conductivity of solid wood and air. According to Zombori [8] this approach is also applicable to wood particle or fibre mats, but has not been validated yet for materials other than OSB.

Both Dai *et al.* [7] and Zombori [8] used geometrical models to describe the structure of the strand mat. Advantages of such approach are that analytical solutions may be available which directly relate geometrical parameters to heat and mass transfer properties. For many applications this approach is certainly appropriate; however, it has to be questioned how well such models describe the complexity of real networks, particularly when coming to fibrous materials. Irregularities in the mat structure like the existence of fibre bundles and the still not well understood deformation processes of individual fibres during consolidation may suggest using complete geometrical information of the mat, rather than simplified models.

Among the first to simulate the permeability of complex wood fibre networks were Koponen *et al.* [9]. For virtual fibrous sheet materials resembling paper and non-woven fabrics they used the lattice-Boltzmann method as computational scheme and showed that it is possible to compute realistic permeability values without free parameters fitted to experimental data.

Only recently Lux *et al.* [10] applied X-ray tomography to determine the structure of low density (170 kg m^{-3}) wood fibre composites, and to compute the macroscopic thermal conductivity from the 3D images of the material by numerical simulation. Due to limits in computational capacity they used a volume averaging technique where the fibres were treated as homogeneous (but anisotropic) elements with properties averaged over the cell-wall material and the cell lumens. A similar approach, but using virtual instead of real fibre networks, has been reported by Faessel *et al.* [11]. They extracted

morphological data of real low density networks (densities up to 250 kg m^{-3}) realized by X-ray micro-tomography and created virtual networks from these morphological data.

The objective of this paper is to present a method to compute the macroscopic permeability and thermal conductivity from the microstructure of wood fibre networks, and to compare the computed properties with experimental data. Using micro-tomography data of relatively high resolution and applying a simulation method that is capable to account for complex geometrical microstructures provides the basis not only for qualitative but quantitative analysis. The whole density range that is relevant to composites for structural applications will be covered, rather than working on insulation materials. Once the method proposed here has been validated for real fibre networks obtained by micro-tomography, it may also be used with sufficient confidence in the future for virtual fibre networks.

2 Material and methods

2.1 Micro-tomography

2.1.1 Sample preparation

Laboratory medium density fibreboard (MDF) samples were prepared from a commercial fibreboard furnish consisting of thermo-mechanical pulp (TMP) softwood fibres (*Pinus sylvestris* L.). The fibres were treated with an urea formaldehyde adhesive (BASF Kaurit 350) in a laboratory blender, resulting in a total resin content of 10% resin solids related to the dry mass of the wood. For forming a mat with horizontally random fibre orientation the wood-furnish was given into a round duct of 100 mm diameter and subsequently pre-pressed. Four MDF samples with a thickness of 5 mm and the diameter of the duct were produced using a computer-controlled miniature hot-pressing system. The pressing program consisted of a 5 s closing step until the target

thickness of 5 mm was reached and a holding stage of 75 s plus an opening stage of 10 s. The samples had a typical cross-sectional density profile, with target average densities ranging from 300 kg m^{-3} to 1000 kg m^{-3}. Samples for micro-tomography investigations with a size of 2 x 2 x 5 mm^3 (length x width x thickness) were cut out and the cutting surfaces were smoothed using razorblades. In this paper the thickness is regarded as the z-direction.

2.1.2 Measurement and 3D image processing

The samples were scanned using synchrotron radiation based X-ray micro-tomography (SRìCT) at the Hamburger Synchrotonstrahlungslabor HASYLAB at Deutsches Elektronen Synchroton DESY in Hamburg, Germany. The measurements of the MDF samples were carried out at a photon energy of 12 keV to match the low absorption of the wood fibres. The magnification was set to 3.98 resulting in an effective pixel size of 2.28 ìm. Each sample was scanned at projection angles from 0° to 180° in steps of 0.25°, leading to 720 projections with a size of 1536 x 1024 pixels. The data were reconstructed to a stack of 2D images with a size of 1536 x 1536 pixels using a filtered-back-projection algorithm. For each sample two scans were recorded, so that a height of 4 mm from one to almost the other sample surface was available for the analysis (Figure 1). Due to the close to symmetrical density profile of the MDF samples, a scan over the entire thickness of the sample was not necessary. The resulting 3D data set had a size of 1536 x 1536 x 2028 voxels (voxel = volumetric pixel), and included some of the air around the MDF sample. The beam time for one sample was approximately five hours.

Due to the huge size of 4 GB for one set of reconstructed 3D greyscale images, only sub-volumes were further processed for noise elimination and segmentation of the voxels into three groups, i.e. cell wall material (grey in Figure 2), cell lumens (black) and inter-fibre voids (white). Cell lumens are defined as being completely separated from inter-fibre voids by cell wall material. To include the whole density range covered by the tomography data for the further analysis, the sub-volumes were extracted from surface layer (labelled I in Figure 1) and intermediate layer positions (i.e., between surface and middle layer, labelled II and III in Figure 1). Each sub-volume had a size of 512 x 512 x 256 voxels. An image processing library (VIGRA) described by Koethe [12] and Koethe [13] was used for the data processing. For a description of the processing steps including those operations to identify individual fibres and fibre bundles the interested reader is referred to Walther *et al.* [14].

2.2 Simulation of physical properties

2.2.1 Permeability

Permeability is a material property that reflects the pore structure of the mat, i.e., the shape and size distribution of the pores. It is independent of the fluid (provided that the fluid does not change the pore structure) and can be expressed by the permeability coefficient. When applying a pressure difference on a porous material the permeability coefficient K in m^{-2} is the proportionality constant between flow velocity u in m s^{-1} and pressure gradient dp/dl in Pa m^{-1}. This relationship can be expressed by Darcy's law that may be written as

$$u = -\frac{K}{\mu}\frac{dp}{dl} \tag{1}$$

where μ in Pa s is the dynamical gas viscosity. Darcy's law is only valid for laminar flow.

Computations of the permeability were done in x-, y- and z-direction of the sub-volumes assuming periodical boundary conditions.

Inter-fibre voids connected to the ambient air, including the air regions inside those fibres that are not completely closed, are accessible for the gas flow. First the geometry of the fibre network is checked for at least one continuous flow path from one to the opposite side of the sub-volume. Only if such a path exists, the further arithmetic procedures are possible. Furthermore, for high densities of the fibre network it is possible that a continuous path through the sub-volume still exists, but that it is interrupted after periodical continuation of the network. That is to say that the periodic boundary conditions would lead to zero permeability even though a path through pore space exists. To overcome this problem the sub-volumes are imbedded into a slightly larger volume, leaving small distances between the sub-volumes. Figure 3 illustrates the issue. On the top, the material geometry that is visible to the flow solver is illustrated by periodic continuation. The white-shaded pores are not connected across the periodic boundaries, due to the low porosity of the specimen. On the bottom, the same periodic continuation is performed, but auxiliary empty space is added in flow direction. Now, pores on opposite faces are always connected through the auxiliary empty space, and the flow solver computes nonzero permeability.

A constant arbitrary pressure difference Δp is assumed between the two surfaces, and the gas velocity u and the gas pressure p is computed for each position within the discretized inter-cellular void system using the Navier-Stokes equation. From the flow field obtained by this procedure the flow resistance and the permeability coefficient,

being the ratio of gas viscosity to flow resistance, is calculated using Darcy's law. Finally, to correct for the slightly enlarged volume the permeability is reduced by the factor $n / (n + n_c)$, where n denotes the total length of the sub-volumes and n_c the total length of the spaces between the sub-volumes.

A comprehensive description of the mathematics involved in computing the permeability is given by Schulz *et al.* [15]. A finite difference solver of the **GeoDict** software (Wiegmann [16]) was used for computations.

2.2.2 Thermal conductivity

Thermal conduction (sometimes referred to as thermal diffusion) is the heat transfer mechanism relying on the energy exchange between neighboring molecules in solids, liquids and gases along a temperature gradient. It is described by Fourier's law that relates the heat flux q in J m^{-2} s^{-1} to the temperature gradient dT / dl in K m^{-1}. Fourier's law may be expressed in the following form

$$q = -\lambda \frac{dT}{dl} \tag{2}$$

Here, the thermal conductivity λ in W m^{-1} K^{-1} is the proportionality constant between heat flux and temperature gradient.

Computations of the thermal conductivity were done for the sub-volumes in x-, y- and z-directions. Only thermal conductivity is considered in this study, but not convective heat transfer and heat radiation.

According to Maku [17] (in Kollmann and Malmquist [18]) the thermal conductivity of the cell wall material parallel and perpendicular to the fibre axis is $\lambda_{w,\parallel}$ = 0.6536 W m^{-1} K^{-1} and $\lambda_{w,\perp}$ = 0.4210 W m^{-1} K^{-1}, respectively. In the simulation of the macroscopic thermal conductivity the anisotropy of the cell wall material is accounted for insofar that the thermal conductivity perpendicular to and within the sample plane was calculated using $\lambda_{w,\perp}$ and $\lambda_{w,\parallel}$, respectively. This convention reflects the

circumstance that the predominant fibre alignment is parallel to the sample plane, while the perpendicular alignment component is more or less negligible even for low density materials. However, in both flow cases thermal conduction through the cell wall material happens, at least to some extend, along the fibre direction and perpendicular to it. Unfortunately it was not possible to account for this with the routines employed.

Air inside the cell lumens and inter-fibre voids was assumed to have a thermal conductivity of $\lambda_a = 0.026$ W m^{-1} K^{-1}. Alternatively, simulation runs were carried out assuming an air thermal conductivity of null. However, these computations resulted in values for the macroscopic thermal conductivity of the samples that considerably deviated from those values obtained experimentally, and will therefore not be further discussed here. Temperature and moisture effects on the thermal conductivity were not considered. Similarly, resin as part of the tested samples is not accounted for in the simulations.

The stationary heat equation is solved with periodic boundary conditions, as it is the case for the permeability problem described above. It is characteristic for the heat flow problem in fibrous networks that one has to deal with high contrast in the thermal conductivities of the two individual phases, namely cell wall material and air. This is achieved by harmonic averaging and explicitly introducing the jumps across the material interfaces as additional variables. The continuity of the heat flux yields the needed extra equations for these variables. The mathematics involved in the simulation and the solver of the **GeoDict** software have been comprehensively described by Wiegmann and Zemitis [19].

2.3 Measurement of physical properties

2.3.1 Sample preparation

To compare the simulated permeability and thermal conductivity coefficients with experimental data, laboratory MDF panels were manufactured from the same wood

fibre material that was used for the micro-tomography samples. A melamine supplemented UF resin (BASF Kaurit 405) was applied to the fibres in a laboratory blender, with an adhesive content of 11 % related to the dry wood. All mats were formed manually aiming for a random alignment of the fibres. The mats were pressed to a target panel thickness of 10 mm for the thermal conductivity measurements and 20 mm for the permeability measurements. The actual densities were somewhat below the target densities of 300, 550, 800 and 1050 kg m^{-3} (based on a moisture content of 10 %), due to the transverse strain of the fibre mats during pressing. Cross-sectional density gradients were widely avoided by pressing the adhesive treated fibre mats at room temperature to its target density and then slowly heating the press with a temperature ramp of 1 to 2°C per minutes. The pressing was stopped when a temperature of 105°C was reached in the core layer.

Cylindrical samples were prepared from the panels, with the main axis perpendicular and parallel to the panel plane for measuring the cross-sectional and within-plane permeability, respectively. The samples to determine the cross-sectional (within-plane) permeability were 18 (30) mm long with a diameter of 47 (15) mm.

For the thermal conductivity measurements, 50 mm wide stripes were sanded from both sides to 4 and 8 mm thickness, respectively, and were subsequently cut into 50 mm long samples. As the measurement of the thermal conductivity through porous materials may be disturbed by a temperature induced moisture transfer from the hot to the cool side, the samples were dried in a drying chamber at 60°C and cooled in a dissicator just until the onset of the measurement. The moisture content of the samples when beginning the measurement was 2.0 % to 2.5 %, and increased by 0.5 % as an average during testing.

2.3.2 Permeability

Care was taken when fitting the samples into the brazing support to avoid air leakages between the sample and the support. Air was passed through the samples at room temperature and the gas pressure in front of and behind the sample was recorded after reaching constant flow conditions for four different preset flow volumes. The pressure difference between the two sides of the sample was kept on a relatively small level to avoid turbulent flow.

The flow velocity can be obtained by dividing the measured flow volume per unit time by the streaming area of the sample. Finally, the permeability coefficient can directly be computed after rearranging equation 1. A complete description of the sample preparation and the permeability measurement is given by Thoemen and Klueppel [3].

2.3.3 Thermal conductivity

A steady-state method was used to experimentally determine the cross-sectional thermal conductivity of the MDF samples. For that a heat flow measuring system (Captec Enterprise Company) with 50 x 50 mm² measuring platens was applied. The samples were placed between the measuring platens, and a constant heat flux perpendicular to the sample plane was generated by an electrically heated source adjacent to one of the measuring platens and an air-cooled sink adjacent to the other platen. The temperature difference between one and the other sample surface was adjusted to about 5°C, and a constant pressing force of 1.6 kPa was applied for all measurements. The surface resistance to the heat flux was accounted for by fitting the overall heat transfer resistance measured for the two different sample thicknesses to a regression line. The intercepts of the lines obtained for different densities give the values for the surface resistances.

3 Results and discussion

3.1 Permeability

According to von Haas *et al.* [1] the relationship between permeability K in m^{-2} and density ρ in kg m^{-3} may be expressed by an equation of the form

$$K = e^{\frac{1}{a+b\rho+c/\ln(\rho)}} \quad (3)$$

where a, b and c are regression coefficients. Fitting the measured cross-sectional and within-plane permeability data to this equation results into the coefficients listed in Table 1.

Curves generated from equation 3 by using the coefficients from Table 1 are displayed in Figure 4, together with the permeability values simulated on basis of the tomography data. The curves cover only that density range where measured data are available; extrapolations are not included in Figure 4.

The thresholds applied during processing of the tomographic data generated some more cell wall material than expected given the cell wall density of 1530 kg m^{-3} and the gravimetrically measured densities of the samples. Therefore, the simulation results are plotted against densities based on the voxel count, rather than against the actual densities of the samples. Please note that for assessing the quality of the flow simulations this deviation of density derived by voxel count and gravimetrically measured density is not critical.

Simulating the permeability based on the tomography date was not possible for those samples of around 1360 kg m^{-3}, as no continuous flow path could be found through the samples any more; the numerical solution of the flow problem converged against zero for such high density samples. The data points for these samples are, therefore, not included in Figure 4.

Considering the fact that the simulations presented here are *ab initio* simulations, with no data fitting involved at all, the agreement between simulation and experimental data can be regarded as promising. Both the simulated and measured sets of permeability data show a similar dependency on the density. The overestimation of the simulated permeability is possibly caused by the still limited resolution of the tomography images, where the typical cell wall thickness is in the order of one or few voxels. The data used for the permeability simulations may omit existing micro-pores and therefore pretend, for a given density, wider flow paths than they actually are. As the permeability of a material for a given density decreases with decreasing pore diameters, a limited resolution will almost certainly lead to an overestimation of the permeability values, provided that such micro-pores exist. Other reasons for differences between simulation and measurement may be inhomogeneities within the samples of investigation, simplified model assumptions, or measuring errors when determining the reference data.

For completeness, simulation runs for the permeability were carried out in two different in-plane directions, i.e. in x- and y-direction. The differences between both directions were found to be statistically insignificant, what was expected before, as there was no predominant alignment direction for the fibres during mat forming. Anticipating this result, measurements of the within-plane permeability were done in only one direction.

For both simulation and measurement the cross-sectional permeability is significantly below the within-plane permeability over the entire density range considered. This finding is in good agreement with results published by v. Haas *et al.* [20], Haselein [21] and Hanvongjirawat [22] for wood fibre materials. Obviously, the horizontal alignment of the fibres in the mat or composite promotes the within-plane flow, compared to the cross-sectional flow.

A comparison of those simulation results obtained for the 512 x 512 x 256 voxel sub-volumes displayed in Figure 4 with results from 256^3 voxel sub-volumes showed almost no differences. Even the smaller grid appears to be large enough for modelling and computing permeability of wood fibre networks.

3.2 Thermal conductivity

By fitting the measured thermal conductivity data to a second order polynomial the relationship between density ρ in kg m^{-3} and cross-sectional thermal conductivity λ in W K^{-1} m^{-1} may be described by the following equation:

$$\lambda = 6.26 x 10^{-8} \rho^2 + 6.20 x 10^{-5} \rho + 5.78 x 10^{-2} \quad (4)$$

The curve in Figure 5 displays the cross-sectional thermal conductivity according to equation 4 for the density range covered by the measurements. No measurements have been conducted for the within-plane thermal conductivity.

The simulated thermal conductivity data available for densities from 500 to 1360 kg m^{-3} based on the voxel count are included in Figure 5. By definition, the macroscopic thermal conductivity approaches those values for the pure cell wall material when coming to a sample density of 1530 kg m^{-3} (not displayed here).

As already found for the permeability data no significant differences can be observed for the simulated thermal conductivity in x- and y-directions. However, the within-plane values are 70 to 110 % higher compared to the cross-sectional (z-direction) ones. One reason for this difference is that the cell wall thermal conductivity as it is employed for the simulations is assumed to be higher in fibre direction than perpendicular to it. However, this differentiation would lead to a with-in plane thermal conductivity that is only 55 % higher than the cross-sectional thermal conductivity. Consequently, part of the difference in macroscopic thermal conductivity must be attributed to the micro-structure of the material. Obviously, the heat flow in fibre

direction is less disturbed by the air-filled and, therefore insulating voids, as it is the case for heat flow perpendicular to the fibres.

Almost all measurements of thermal conductivity for wood-based composites described so far in the literature were done on panels where the main fibre direction was perpendicular to the direction of heat flow. The reason is that the within plane thermal conductivity is typically only of minor importance as an engineering parameter. Besides, the experimental setup for the cross-sectional case is more straightforward than for the latter one. However, Humphrey and Bolton [23] estimated from data obtained by Ward and Skaar [24] and from their own preliminary measurements that the thermal conductivity of particleboards parallel to the main fibre direction is about 50 % higher than for the cross-sectional thermal conductivity. For fibreboards no such data are known from the literature. The simulated values presented in Figure 5 indicate that for MDF the thermal conductivity within the panel plane is approximately twice as high as perpendicular to it, and not only 50 % higher as it was estimated by Humphrey and Bolton [23] for particleboard.

Reasonably good agreement was found when comparing simulated and measured cross-sectional thermal conductivity, and the quadratic form of the relationship between thermal conductivity and density could be confirmed by the simulations. The discrepancies still noticeable may, as already mentioned with respect to the permeability data, be allocated to inhomogenities within the samples, some simplifications in the model assumptions and measuring errors when experimentally determining the thermal conductivity.

4 Conclusions

In this paper an approach is presented to compute macroscopic permeability and thermal conductivity of a wood fibre network from its microstructure. This approach

uses numerical methods to solve the respective set of equations, and does not include any free parameters to fit the simulation results to experimental data.

In principle, the approach presented here is not limited to images of real fibre networks, such as tomography data, but can also be applied to complex virtual fibre networks that are generated on a computer. Such virtual networks for MDF type of materials have already been presented in the past, for example by Wang and Shaler [25], but have not been used for simulating transfer properties. The advantage of using virtual networks to simulate the properties of composite materials is evident; no experimental efforts are required for sample preparation and tomographic measurements, providing a fast and inexpensive way to link structural parameters to transfer properties.

It is demonstrated in this research that the simulation results correspond well with experimental data. This validation of the simulation method is important if we want to apply it with sufficient confidence to virtual fibre networks. Having a method to easily and reliably simulate permeability and thermal conductivity of fibre networks generated on the computer opens a range of opportunities in research and development:

- The relationship between the structure of the semi-manufactured network (e.g., the wood-furnish mat prior to hot-pressing) on the one hand and its transport properties can be analyzed. Such information may be used to optimize the geometry and organization of the fibres, particles or strands, respectively, and the processes to manufacture them.

- As the transport properties, in turn, directly influence the further processing steps, the simulation approach presented in this paper may be linked to simulation models of the subsequent sub-processes. For example, if we link the model for the transport properties to a hot-pressing model we can directly analyze the effects of fibre geometries and organization on the performance of the mat inside the hot press, and possibly on the properties of the final product. All hot pressing models for MDF and

particleboard presented so far (Carvalho and Costa [26], Garcia and Cloutier [2], Thoemen and Humphrey [27]) use empirically derived expressions to describe the transport properties of the wood-furnish mat as input parameters, but do not include the simulation of these properties from the mat structure.

- Processes others than the wood-based panel may be investigated. For example, the fibre packing, geometries and orientation in the resin transfer molding (RTM) process influence the permeability of the fibre bed and hence the maximum fibre content in the composite. Simulation tools to compute the flow pattern in the RTM process may help to optimize the fibre material.

- Conclusions can be drawn on how to design building products with optimized transport properties. So far, most of the information on the effects on the performance of such materials is rather empirical in nature, but not much is know about the link between the microstructure and the material properties.

While those approaches using geometrical models to describe the structure of the wood-furnish mat generate results that are readily integrated into a constitutive analytical model, and hence provide a more direct link between geometrical parameters of the mat and the transport properties, the approach presented here has the advantage of being capable to treat close to reality mat structures instead of simplified ones. Inhomogeneties in the fibre network introduced by irregular structures of fibre bundles, local material agglomerations, reinforcement fibres or contaminants can be fully accounted for.

There were no free parameters in the simulations which would have been used for fitting with the experimental results. That is to say that an *ab initio* simulation method has been introduced here, where new material designs that have not been realized by experiment, so far, can be investigated regarding their physical properties. Such capability opens new possibilities in design and optimization of natural fibre based

composites. While the focus in this paper was on permeability and thermal conductivity, this approach may also be suitable to simulate other physical properties of natural fibre-based materials, such as the gas diffusion coefficient, electrical conductivity or acoustical properties.

Acknowledgements

The authors gratefully acknowledge support of this work by the Arthur and Aenne Feindt Foundation. They also would like to express their thanks to the GKSS Research Centre at HASYLAB, Hamburg, Germany, for letting them use their SRμCT equipment, and to the Kaiserslautern Excellence Cluster Dependable Adaptive Systems and Mathematical Modeling for their support.

Literature

1. von Haas G, Steffen A, Fruehwald A. Untersuchungen zur Permeabilität von Faser-, Span- und OSB-Matten für Gase. Holz als Roh- und Werkstoff 1998; 56(6): 386-392.
2. Garcia RA, Cloutier A. Characterization of heat and mass transfer in the mat during the hot pressing of MDF panels. Wood and Fiber Science 2005; 37(1): 23-41.
3. Thoemen H, Klueppel A. Investigations on the permeability of different wood furnish materials. Holzforschung (in preparation).
4. Shao M. Thermal properties of wood fiber networks. M.S. Thesis, Oregon State Univ. 1989: 95 pp.
5. von Haas G. Untersuchungen zur Wärmeleitfähigkeit von Faser- und Spanmatten und Platten. Holzforschung und Holzverwertung 2000; 52(5): 102-104.
6. Klueppel A. Vergleichende Charakterisierung von Faser- und Spanmatten zur Herstellung von Holzwerkstoffen unter besonderer Berücksichtigung der Permeabilität und Wärmeleitfähigkeit. Diploma Thesis, University of Hamburg, Department of Biology, 2006.
7. Dai CP, Yu CM, Zhou XY. Heat and mass transfer in wood composite panels during hot pressing. Part II. Modeling void formation and mat permeability. Wood and Fiber Science 2005; 37(2): 242-257.
8. Zombori BG. Modeling the Transient Effects during the Hot-Compression of Wood-Based CompositesThesis, Virginia State University, 2001.

9. Koponen A, Kandhai D, Hellén E, Alava M, Hoekstra A, Kataja M, Niskanen K, Sloot P, Timonen J. Permeability of Three-Dimensional Random Fiber Webs. The American Physical Society 1998; 80(4): 716-719.

10. Lux J, Delisée C, Thibault X. 3D characterization of wood based fibrous materials: an application. Image Anal Stereol 2006; 25: 25-35.

11. Faessel M, Delisée C, Bos F, Castéra P. 3D modelling of random cellulosic fibrous networks based on X-ray tomography and image analysis. Composites Science and Technology 2005; 65: 1931-1940.

12. Koethe U. Reusable software in computer vision. In: B. Jähne, H. Haussecker, and P. Geissler, editors. Handbook of computer vision and applications, vol. 3: Systems and applications. San Diego: Academic Press, 1999.

13. Koethe U. STL-style generic programming with images. C++ Report Magazine 2000; 12(1): 24-30.

14. Walther T, Terzic K, Donath K, Meine H, Beckmann F, Thoemen H. Microstructural analysis of lignocellulosic fiber networks. Proceedings of Conference on Developments in X-Ray Tomography V, SPIE Volume 6318, CID Number 631812. 13.-17.08.2006. San Diego, California, USA.

15. Schulz V, Kehrwald D, Wiegmann A, Steiner K. Flow, heat conductivity, and gas diffusion in partly saturated microstructures. Proceedings of NAFEMS CFD Seminar: Simulation of Complex Flows. Niedernhausen/Wiesbaden, Germany, 25.-26.04.2005: NAFEMS, Grafing near Munich, Germany.

16. Wiegmann A. A fast fictitious force 3d-Stokes solver. (in preparation).

17. Maku T. Studies on the heat conduction in wood. Wood Res. Bulletin, Kyoto Univ., Japan 1954; 13: 1-80.

18. Kollmann F, Malmquist L. Ueber die Waermeleitzahl von Holz und Holzwerkstoffen. Holz als Roh- und Werkstoff 1956; 14(6): 201-204.

19. Wiegmann A, Zemitis A. EJ-HEAT: A Fast Explicit Jump Harmonic Averaging Solver for the Effective Heat Conductivity of Composite Materials. Fraunhofer ITWM: 94, Kaiserslautern, Germany, 2006.

20. v. Haas G, Steffen A, Frühwald A. Untersuchungen zur Permeabilität von Faser-, Span- und OSB-Matten für Gase. Holz als Roh- und Werkstoff 1998; 56(6): 386-392.

21. Haselein CR. Numerical simulation of pressing wood-fiber composites. PhD Thesis, Oregon State University, Forest Products Department, 1998.

22. Hanvongjirawat W. Permeabilitaet von Holzwerkstoffmatten. PhD Thesis, University of Hamburg, Faculty of Biology, 2003.

23. Humphrey PE, Bolton AJ. The hot pressing of dry-formed wood-based composites. Part II: A simulation model for heat and moisture transfer. Holzforschung 1989; 43(3): 199-206.

24. Ward RJ, Skaar C. Specific heat and conductivity of particleboard as functions of temperature. Forest Products Journal 1963; 13(1): 31-38.

25. Wang H, Shaler SM. Computer-Simulated Three-Dimensional Microstructure of Wood Fibre Composite Materials. Journal of Pulp and Paper Science 1998; 24(10): 314-319.

26. Carvalho LMH, Costa CAV. Modeling and simulation of the hot-pressing process in the production of medium density fiberboard (MDF). Chemical Engineering Communications, Gordon & Breach Science Publ Inc 1998; 170: 1-21.

27. Thoemen H, Humphrey PE. Modeling the physical processes relevant during hot pressing of wood-based composites. Part I. Heat and mass transfer. Holz als Roh- und Werkstoff 2006; 64(1): 1-10.

Figures captions

Figure 1: Reconstructed 3D-Volume of a MDF sample with a density of 300 kg m^{-3}. Locations of the sub-volumes chosen for further data processing are numbered from I to III.

Figure 2: Slices through x-y (left) and y-z (right) plane after noise elimination and segmentation into cell-wall material (grey), cell lumens (black) and inter-fibre voids (white).

Figure 3: Schematic to illustrate the periodic continuation of a sub-volume in one dimension. Top: No empty space between the replications. Bottom: Sub-volumes imbedded into a slightly larger volume.

Figure 4: Mat permeability obtained by *ab initio* simulations (symbols) and by fitting curves to experimental data (lines).

Figure 5: Thermal conductivity obtained by *ab initio* simulations (symbols) and by fitting curves to experimental data (line).

Tables

Table 1. Regression coefficients from fitting experimental permeability data for MDF to equation 3

	a	b	c	R^2
cross-sectional permeability	-0.025	7.88×10^{-6}	-0.106	0.998
within-plane permeability	-0.025	7.02×10^{-6}	-0.101	0.998

Fig 1:

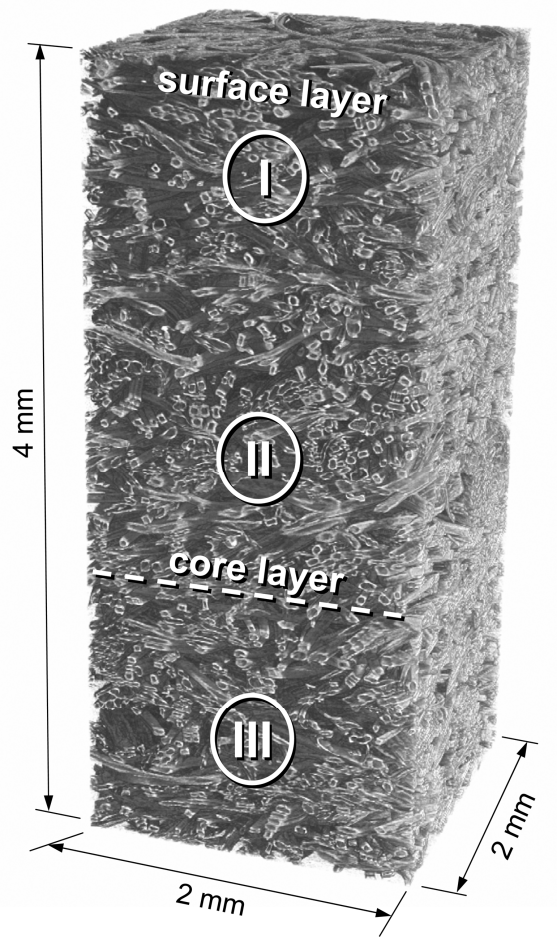

Fig 2:

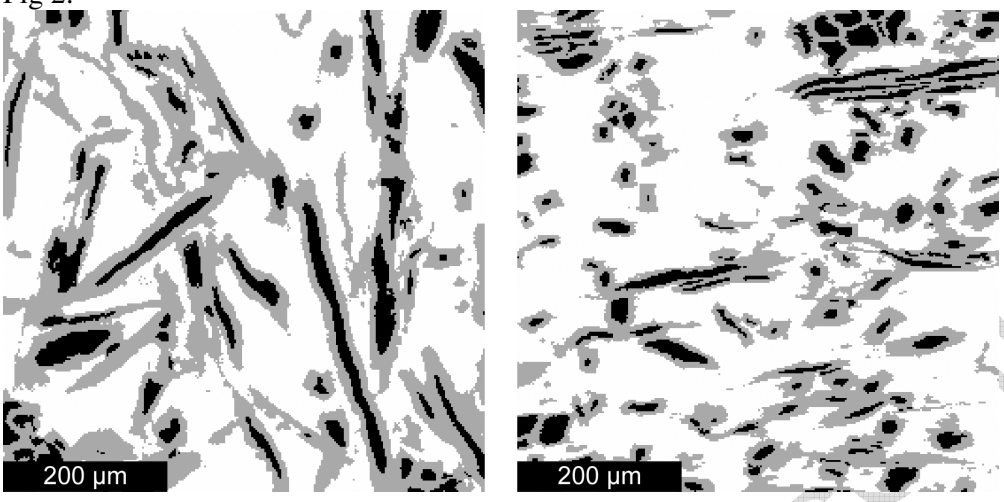

Fig 3:

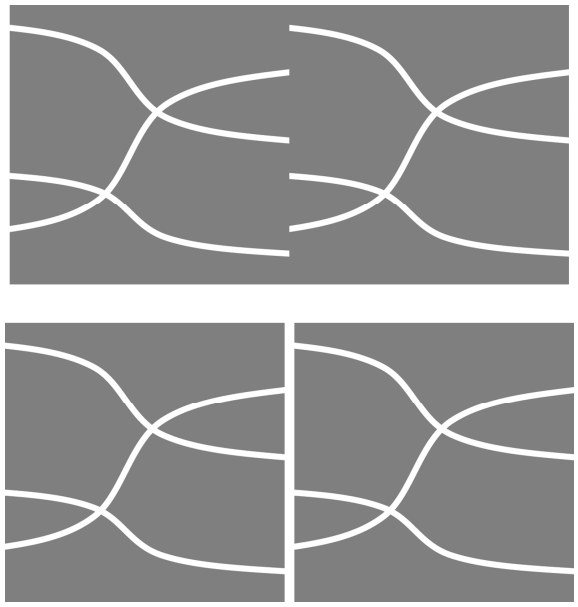

Fig 4:

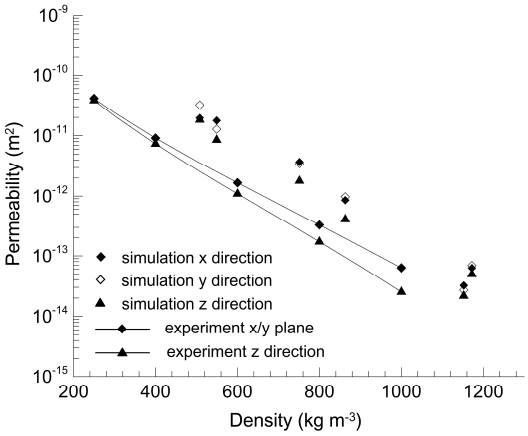

Fig 5: